Asphericity in the magnetization distribution of holmium*

G. P. Felcher,† G. H. Lander, and T. Arai
Argonne National Laboratory, Argonne, Illinois 60439

S. K. Sinha‡ and F. H. Spedding
Ames Laboratory, Ames, Iowa 50010

(Received 3 November 1975)

In a spiral magnetic structure an aspherical magnetic moment distribution around the ions gives rise to a new set of diffraction lines indexed as third-order satellites. Neutron-diffraction measurements have been made on single crystals of holmium and a $Ho_{0.9}Sc_{0.1}$ alloy to determine the magnetic structures as a function of temperature, and measure the intensities of the third-order satellites. From these intensities the experimental asphericity of the magnetization density is compared to that calculated with a single-ion model. The agreement between theory and experiment is qualitative; the experimental intensities being larger by a factor of ~ 1.5. The temperature dependence of the third-order satellite is in good agreement with a simple model proposing exchange splitting of the free-ion multiplet, with a negligible crystal-field interaction.

I. INTRODUCTION

Most of the magnetic properties of the heavy-rare-earth metals are well accounted for by assuming that the $4f$ electrons are shielded from the neighboring atoms, and that their large spin-orbit interaction leads to Russell-Saunders coupling. Following Hund's rule the ground state for holmium should therefore be described by the spectroscopic state $^5I_8$, with an ordered moment of $10.0\mu_B$. The strong spin-orbit coupling means that the unique axis of the magnetization distribution is usually defined by the moment direction $\vec{J}$ rather than by the crystal field. In contrast, the aspherical spin densities in the transition series are determined primarily by the crystal field. The measurement of the asphericity of the moment distribution of the rare earths in a solid can provide a test of the validity of this "atomic" picture.

As is well known, the asphericity of the magnetization can be investigated by measuring the magnetic scattering amplitudes as a function of $\vec{\kappa}$, the scattering vector. In general, these amplitudes are sensitive to both the spherical and aspherical parts of the magnetization density, the aspherical part usually being the smaller of the two. In this paper we report an alternative method, first suggested for spiral structures by Blume,[1] that measures only the aspherical contribution to the magnetization density. As a consequence of the spin-orbit interaction, both the charge and magnetization density associated with the $4f$ electrons are aspherical. The charge asphericity has been the subject of a very careful x-ray experiment by Keating.[2] In a sense the present experiment is a complementary one, but, because the theory is less complex and the effects much larger in the neutron case, a more quantitative comparison can be made with theory.

In Sec. II of this paper, an account is given of how the asphericity gives rise to new set of coherent diffraction lines from a spiral magnetic structure. In Sec. III, the magnetic structure of Ho and $Ho_{0.9}Sc_{0.1}$ is reviewed. In Sec. IV, the experimental results obtained for the asphericity of the magnetization density are presented and discussed.

II. ASPHERICITY AND THE SPIRAL STRUCTURE

Using the tensor approach[3] the magnetic form factor of a rare-earth ion in a given $|SLJM\rangle$ state can be written as

$$f(\vec{\kappa},\beta) = \frac{1}{|\mu|\sin^2\beta}\sum_{n=0}^{3} X_{2n}(\beta)(c_{2n+1}\langle j_{2n}\rangle + c_{2n+2}\langle j_{2n+2}\rangle), \tag{1}$$

where β is the angle between the direction of the magnetic moment $\vec{\mu}$ and the scattering vector $\vec{\kappa}$. The magnetic form factor is expressed in Eq. (1) in terms of the Bessel transforms of the spin-density distribution:

$$\langle j_{2n}\rangle = \int_0^\infty U(r) j_{2n}(\kappa r)\, dr, \tag{2}$$

where $U(r)$ is the radial spin-density distribution of the $4f$ electrons, and $j_{2n}(\kappa r)$ is the spherical Bessel function. The terms $\langle j_{2n}\rangle$ have been calculated by the Hartree-Fock method[4] for the complete $4f$ series and are presented for holmium in Fig. 1. The coefficients c_n appearing in Eq. (1) are constants, characteristic of the $|SLJM\rangle$ state. They have been reported[5] for all rare earths for $M=J$ and are given for all states of the lowest

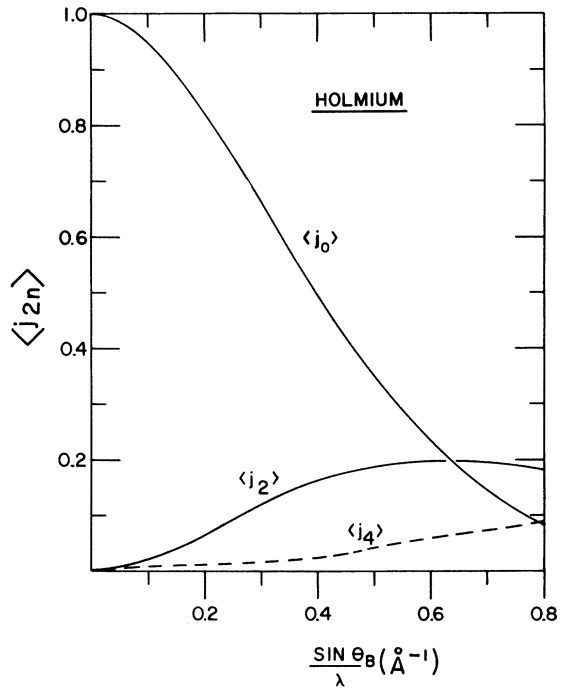

FIG. 1. $\langle j_{2n}\rangle$ functions of holmium as given by Blume *et al.* (Ref. 4). (The $\langle j_6\rangle$ function is less than $\frac{1}{2}$ of $\langle j_4\rangle$ in this range of $\sin\theta_B/\lambda$.)

multiplet of holmium in Table I. The coefficients X_{2n} in Eq. (1) indicate the angular dependence of the magnetic form factor, as expressed by

$$X_{2n}=2\left(\frac{(2n+1)(2n+2)}{4n+3}\right)^{1/2}[P_{2n}(\cos\beta)-P_{2n+2}(\cos\beta)], \tag{3}$$

where P_{2n} are Legendre polynomials. Both the coefficients c_n and the transforms $\langle j_n\rangle$ rapidly decrease in magnitude with the increase of their order; the lowest term represents the main portion of the spherically averaged form factor and higher terms describe the asphericity of the magnetization cloud.

The terms in Eq. (1) may be rearranged to demonstrate the dependence of the form factor on the angle β. By expanding the Legendre polynomials in Eq. (3), we obtain from Eq. (1).

$$f(\vec{\kappa},\beta)=\sum_{n=0}^{3}A_{2n}(\kappa)\cos(2n\beta), \tag{4}$$

where the coefficients A_{2n} are linear functions of the c_n and $\langle j_n\rangle$, with the leading contribution given by c_{2n+1} and $\langle j_{2n}\rangle$ (Table II). The A_{2n} terms also rapidly decrease with increase of order n.

In Eq. (4) the spherical ($n=0$) and the aspherical contributions to the form factor are well separated. If each of the terms A_{2n} could be measured independently a considerable amount of information about the electronic state of the system could be obtained. Such a separation is indeed possible if the magnetic moments are arranged in a spiral structure.[1] In such a magnetic structure the magnitude cross section is proportional to

$$\frac{d\sigma}{d\Omega}\propto\left(\sum_L\frac{\vec{\mu}_x-i\vec{\mu}_y}{2}f(\vec{\kappa},\beta_L)e^{i\phi_L}+\sum_L\frac{\vec{\mu}_x+i\vec{\mu}_y}{2}f^*(\vec{\kappa},\beta_L)e^{-i\phi_L}\right)^2. \tag{5}$$

All the magnetic moments lie in a plane; the structure consists of ferromagnetic layers, with the moments on the Lth layer at an angle ϕ_L from a projection of $\vec{\kappa}$, the scattering vector, on the ferromagnetic layers. The form factor in Eq. (5) can also be expressed in terms of ϕ_L, by using the simple transformation property

$$\cos\beta_L=\cos\theta\cos\phi_L, \tag{6}$$

where θ is the azimuth of the scattering vector from the plane of the spiral; see Fig. 2. (Note that we use θ_B for the Bragg angle to avoid confusion.) Equation (4) then takes the form

$$f(\vec{\kappa},\beta_L)=\sum_{n=0}^{3}B_{2n}(\kappa,\theta)\cos(2n\phi_L), \tag{7}$$

where the terms B_{2n} are obtained from the coefficients A_{2n} by a simple geometrical transformation (Table II). The coefficients B_{2n} retain the main

TABLE I. Coefficients c_n for holmium in the magnetic state $^5I_8$. (To compare with Table II of Ref. 5 multiply by $\sqrt{6}$.)

M	c_1	c_2	c_3	c_4	c_5	c_6	c_7
8	4.0825	2.5039	−0.3055	−0.2777	+0.1251	+0.1463	−0.1126
7	3.5722	2.1909	−0.0764	−0.0694	−0.1095	−0.1280	+0.2815
6	3.0618	1.8779	+0.0764	+0.0694	−0.1251	−0.1463	−0.0338
5	2.5515	1.5649	+0.1637	+0.1488	−0.0469	−0.0549	−0.2139
4	2.0412	1.2519	+0.1964	+0.1785	+0.0433	+0.0506	−0.1291
3	1.5309	0.9390	+0.1855	+0.1686	+0.0999	+0.1167	+0.0650
2	1.0206	0.6260	+0.1418	+0.1290	+0.1059	+0.1238	+0.1862
1	0.5103	0.3130	+0.0764	+0.0694	+0.0662	+0.0774	+0.1516

TABLE II. Coefficients A_{2n} and B_{2n}.

$$A_0 = (2.450c_1)\langle j_0\rangle + (2.450c_2 + 3.435c_3)\langle j_2\rangle + (3.435c_4 + 4.256c_5)\langle j_4\rangle + (4.256c_6 + 4.954c_7)\langle j_6\rangle$$
$$A_2 = (5.725c_3)\langle j_2\rangle + (5.725c_4 + 7.945c_5)\langle j_4\rangle + (7.945c_6 + 9.552c_7)\langle j_6\rangle$$
$$A_4 = (5.960c_5)\langle j_4\rangle + (5.960c_6 + 5.386c_7)\langle j_6\rangle$$
$$A_6 = (6.070c_7)\langle j_6\rangle$$

$$B_0 = A_0 - A_2\sin^2\theta + A_4(24\cos^4\theta - 4\cos^2\theta + 1) + A_6(136\cos^6\theta - 144\cos^4\theta + 9\cos^2\theta - 1)$$
$$B_2 = A_2\cos^2\theta - A_4(4\sin^2\theta)\cos^2\theta + A_6(15\cos^4\theta - 24\cos^2\theta + 9)\cos^2\theta$$
$$B_4 = A_4\cos^4\theta - A_6(6\sin^2\theta)\cos^4\theta$$
$$B_6 = A_6\cos^6\theta$$

properties of the A_{2n}; i.e., their leading contribution is given by c_{2n+1} and $\langle j_{2n}\rangle$. Approximately, B_0 represents the spherical component of the form factor and is isotropic. The term B_2 represents the leading aspherical term and is proportional to $\cos^2\theta$. Substituting Eq. (7) in Eq. (5), the magnetic moments of the Lth layer of a spiral structure can be expressed as

$$\vec{\mu}_L f(\vec{\kappa},\beta_L) = \frac{\vec{\mu}_x - i\vec{\mu}_y}{2}\left(B_0 e^{i\phi_L} + \frac{B_2}{2}e^{-i\phi_L} + \frac{B_2}{2}e^{3i\phi_L} + \frac{B_4}{2}e^{-3i\phi_L} + \frac{B_4}{2}e^{5i\phi_L} + \frac{B_6}{2}e^{-5i\phi_L} + \frac{B_6}{2}e^{7i\phi_L}\right)$$
$$+ (\text{complex conjugate terms}). \tag{8}$$

The spiral is simple when $\phi_L = \vec{\tau}\cdot\vec{R}_L$, with $\vec{\tau}$ the propagation vector of the spiral (normal to the plane of the magnetic moment) and $\vec{R}_L$ the position of the Lth cell. The structure factor for the system can be obtained from Eq. (8) by calculating the magnetic scattering amplitude associated with each magnetic moment, summing over all magnetic moments, and averaging over the neutron states. The final expression for the square of the structure factor, in barns, is

$$|F|^2 = 0.0725\,\mu^2\frac{1+\sin^2\theta}{4}\left[\left(B_0^2 + \frac{B_2^2}{4}\right)\delta_{\vec{Q}_{hkl}\pm\vec{\tau},\vec{\kappa}} + \left(\frac{B_2^2}{4} + \frac{B_4^2}{4}\right)\delta_{\vec{Q}_{hkl}\pm 3\vec{\tau},\vec{\kappa}} + \left(\frac{B_4^2}{4} + \frac{B_6^2}{4}\right)\delta_{\vec{Q}_{hkl}\pm 5\vec{\tau},\vec{\kappa}} + \left(\frac{B_6^2}{4}\right)\delta_{\vec{Q}_{hkl}\pm 7\vec{\tau},\vec{\kappa}}\right], \tag{9}$$

where $\vec{Q}_{hkl}$ is a general reciprocal-lattice vector.

The first term on the right-hand side of Eq. (9) represents the diffraction lines (satellites) that are present even if the distribution of magnetization around each atom is spherically symmetric. The additional diffraction lines are due to the aspherical terms of the magnetization density. The intensity of these terms is small compared to the leading one; even for the most aspherical ions in the ground state the ratio $I_{2|n|+1}/I_{2|n|-1}$ is of the order of 10^{-2}–10^{-4}, depending upon the magnitude of κ. However, the intensities of the third-order satellites appearing at $\vec{Q}_{hkl}\pm 3\vec{\tau}$ can be detected and have characteristics that determine their origin as the asphericity of the ion. First, the leading Bessel transform contained in these terms is $\langle j_2\rangle$, which goes to zero for $\kappa \to 0$, whereas for structural satellites (as we shall refer to satellites arising from the spherical components of the magnetization) the leading term is $\langle j_0\rangle$, which increases as $\kappa \to 0$. Second, the intensities of the third-order satellites drop to zero when the scattering vector is normal to the plane of the spiral, $\theta = \pi/2$. Again, this is in contrast with the behavior of the structural satellites.

So far, we have discussed the diffraction effects from ideal spiral structures. In practice, magnetic spiral structures are seldom so simple, usually exhibiting higher-order modulations that result in additional diffraction effects. Such modulations, which can arise from crystal-field or other anisotropic two-ion interactions, may give rise to additional structural satellites which may coincide with the third-order satellites arising from the intrinsic single-ion asphericity. Of course, associated with every modulation of the spiral structure will be further satellites arising from the single-ion asphericity. As discussed previously these will be much weaker (by factors of 10^{-2}–10^{-4}) than the structural satellites, so they

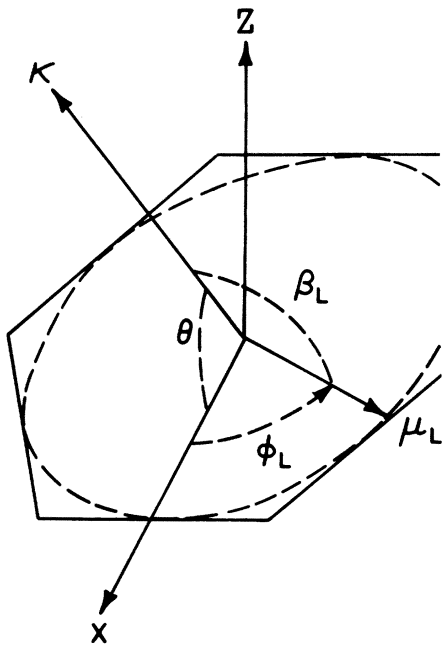

FIG. 2. Transformation of the angle β_L between the scattering vector $\vec{\kappa}$ and the moment direction $\vec{\mu}_L$ in terms of the azimuthal angle θ and the turn angle ϕ_L of the spiral at the Lth layer.

may be extremely difficult to observe. The successive complications that may arise in the diffraction pattern are illustrated schematically in Fig. 3. To study the asphericity of the $4f$ magnetization distribution, the magnetic ions must not be spherically symmetric and the magnetic moments must be arranged in a spiral configuration. These conditions are best fulfilled for pure holmium. At low temperatures, however, the magnetic structure of holmium is not a simple spiral.[6] Initially we had hoped that by diluting holmium with scandium a simple spiral could be obtained. As we shall see, this hope was unfulfilled. Most of the experiment was done on a $Ho_{0.9}Sc_{0.1}$ alloy, with a few checks on pure holmium. In view of the importance of the magnetic structure on the determination of the asphericity parameters, the magnetic structures of Ho and $Ho_{0.9}Sc_{0.1}$ are reviewed in Sec. III.

III. MAGNETIC STRUCTURE

A. Previous work

The magnetic structure of holmium has been the subject of extensive research by Koehler *et al.*[6] Holmium has the hexagonal-close-packed atomic structure and is antiferromagnetic below 133 K. The magnetic structure is a simple spiral down to ~50 K, with the propagation vector along the c axis. Between 133 and ~50 K only first-order

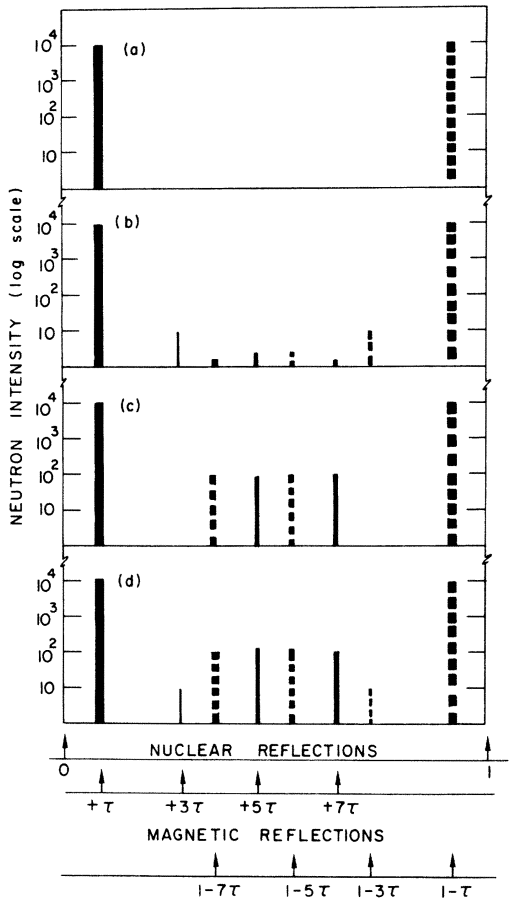

FIG. 3. Representation of some magnetic satellites along the c^* line of reciprocal space. In (a) first-order satellites from the spiral structure appear at $+\tau$ and $-\tau$ from the nuclear positions (denoted by 0 and 1). In (b) the aspherical magnetization density leads to third-, fifth-, and seventh-order satellites. In (c) the effects of bunching in the basal plane lead to fifth- and seventh-order satellites. In (d) the total effects are represented.

satellites were observed, Below 50 K weak additional fifth- and seventh-order satellites were observed. At 4.2 K the intensity of these satellites was about 10^{-2} times the intensity of the main satellites. Their presence was interpreted as due to a bunching of the magnetic moments in the hexagonal plane, a torque effect from the term P_6^6 of the hexagonal anisotropy (Fig. 4). In the bunched structure, the angle of the Lth magnetic moment with the hard hexagonal axes is given by

$$\phi_L = \phi_L^0 + \gamma \sin 6\phi_L^0 + \cdots, \tag{10}$$

where $\phi_L^0 = \vec{\tau} \cdot \vec{R}$, with $\vec{\tau}$ the propagation vector of the unmodulated spiral. The Lth magnetic moment is given, approximately, by

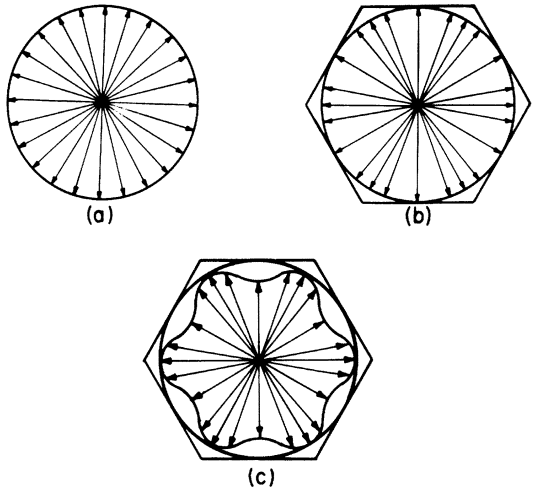

FIG. 4. Projections of (a) simple spiral, (b) bunched spiral, and (c) a bunched spiral with a moment modulation.

$$\vec{\mu}_L = \frac{\vec{\mu}_x - i\vec{\mu}_y}{2}\left(e^{i\vec{\tau}\cdot\vec{R}_L} - \frac{\gamma}{2}e^{-5i\vec{\tau}\cdot\vec{R}_L} + \frac{\gamma}{2}e^{7i\vec{\tau}\cdot\vec{R}_L} + \cdots\right) + \text{c.c.} \qquad (11)$$

This modulation of the magnetic moment directions gives rise, by a procedure similar to that used to obtain Eq. (9) from Eq. (8), to fifth- and seventh-order satellites with intensities proportional to $\gamma^2/4$. Below 20 K the magnetic structure changes from a spiral to a shallow cone with a ferromagnetic component along the c axis. The projection of the cone in the hexagonal plane still retains the characteristics of the bunched structure.

Much less work has been done on the alloy $Ho_{0.9}Sc_{0.1}$, previously available only in powder form, although the magnetic structure is known to be a spiral.[7]

B. Experiments

The experiments on $Ho_{0.9}Sc_{0.1}$ were performed with a single crystal cut in the shape of a parallelepiped with dimensions $0.7 \times 1.4 \times 12$ mm^3. The longest dimension was parallel to a [10.0] axis, the shortest parallel to a [11.0]. The crystal was mounted with the longest axis perpendicular to the scattering plane, measurements being limited to $(hh.l)$-type reflections. The scandium content was analyzed as 9.2 at.%, with no other major impurities present. The intensity measurements were made with the neutron diffractometer at the Ames Laboratory Research Reactor. The incident wavelength was 1.18 Å, obtained from the (103) planes of a beryllium monochromator, with a collimation of 10-min arc before the sample.

The sample of holmium was cut from the large single crystal used by Keating.[2] Its dimensions were $0.8 \times 0.8 \times 8$ mm^3, again with the longest axis parallel to [10.0] axis, and the other two parallel to the [11.0] and the [00.1] directions. Experiments on pure holmium were performed at the CP-5 reactor at Argonne National Laboratory. The wavelength was 1.059 Å, obtained from the (002) plane of a beryllium monochromator. The initial sample was not magnetically homogeneous, since at 4.2 K two series of magnetic satellites with different pitch parameter were observed. The inhomogeneity was removed by annealing for one day at 600 °C.

Absorption, Debye-Waller, and extinction corrections were made to the integrated intensities. The absorption corrections calculated with the standard Busing and Levy program[8] were small, with transmission factors ~90%. At 4.2 K the Debye-Waller correction is also small (~5%), and a value of $B = 0.1$ Å^2 has been used to calculate the temperature factor. The extinction corrections are considerably more uncertain, and were estimated from the variation of the nuclear intensities and from the temperature dependence of the magnetic intensities. For example, the 00.2^- and 22.0^+ reflections both arise from the main spiral component, so that the ratio of their intensities (approximately 30) should be independent of temperature. However, as the ordered moment increases both reflections increase in intensity and will be disproportionately affected by extinction. Using the Zachariasen approach[9] the intensity is reduced by the factor $y = 1/(1 + 2gQt)^{1/2}$, where Q is the crystal reflectivity, t the path length, and g the extinction factor. The extinction factors y were found in the most severe cases to be ~0.8. The magnetic intensities have been placed on an absolute scale by using mean nuclear coherent scattering lengths of $b = 0.88 \times 10^{-12}$ and 0.85×10^{-12} cm for $Ho_{0.9}Sc_{0.1}$ and Ho, respectively. Multiple scattering effects were examined very carefully, since triple scattering of the fundamental magnetic satellites can give rise to spurious satellites of third order. The double scattering effects were calculated, and fitted semiquantitatively to the very weak experimental intensities appearing at the required positions. From these the triple scattering was calculated and found to be negligible. A novel diffraction effect, stemming from the intrinsic multiple scattering of the innermost satellites, was also found.[10]

C. Results

The magnetic structure of both holmium and $Ho_{0.9}Sc_{0.1}$ can be well described by the model pro-

TABLE III. Magnetic properties of Ho and $Ho_{0.9}Sc_{0.1}$.

Description	$Ho_{0.9}Sc_{0.1}$	Ho (annealed)	Ho (sample B, Koehler)
Transition temperatures:			
$T_{Néel}$(K)	115		133
$T_{Bunching}$ [a] (K)	35	~42	~42
$T_{I\text{-}ferromagnet}$(K)	15 ±1	20 ±1	19.0±1
Parameters at 4.2 K:			
ω, turn angle (deg)	41.6 ±0.2	33.3 ±0.2	30.0
μ_F, ferromagnetic component (μ_B)	1.6 ±0.1	1.7 ±0.1	1.7
θ_F, cone angle (deg)	9.2 ±0.5	9.8 ±0.5	9.8
γ (bunching)	0.15±0.01	0.144±0.003	0.16
$\Delta\mu/\mu$ (moment defect)	0.03±0.01	0.019±0.003	•••

[a] $T_{Bunching}$ is the temperature at which the bunching starts to be visible in the diffraction pattern, and does not correspond to a transition point.

posed by Koehler.[6] We give a summary of the magnetic structural properties of the two samples in Table III. Some of the low-temperature parameters of our sample of holmium, notably the pitch of the spiral, do not agree with those given by Koehler, presumably because these parameters are sample dependent.[6]

In the analysis of the magnetic intensities, some features were found that suggest a further refinement of the Koehler's model. The "reduced intensities"—as we call the quantities $|F|^2/[(0.2695f)^2(1+\cos^2\theta)]$—of the fifth and the seventh satellites are not equal, but $I_5 \sim 2I_7$ as shown in Fig. 5 for the pure-Ho sample. Very similar results were obtained for the $Ho_{0.9}Sc_{0.1}$ alloy. According to the description of the bunching given in Eqs. (10) and (11), and in Ref. 6, the reduced intensities for both satellites should be equal to $\gamma^2/4$ in the first approximation. The introduction of higher-order terms in the expression can indeed make the reduced intensities of the two satellites slightly different; however, such higher-order effects cannot produce a factor of 2.

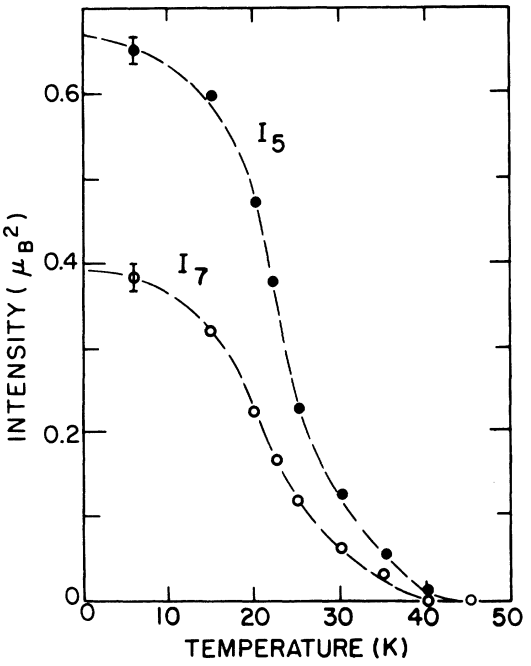

FIG. 5. Reduced intensities $|F|^2/[(0.2695f)^2(1+\cos^2\theta)]$ of the fifth- and seventh-order satellites in Ho as a function of temperature.

The bunching illustrated in Fig. 4(b) is a result of the crystal-field interaction that produces easy and hard axes in the hexagonal basal plane. One might argue that a secondary effect, in which the projection of the moment in the hard direction is reduced in intensity, could also occur. Such an effect is illustrated in Fig. 4(c). Empirically this reduction in the magnetic moment may be represented by a simple modification of Eq. (11):

$$\phi_L = \phi_L^0 + \gamma \sin 6\phi_L^0 + i(\Delta\mu/\mu)\cos 6\phi_L^0. \qquad (12)$$

The intensities of the fifth and seventh satellites are then proportional to $(\gamma + \Delta\mu/\mu)^2$ and $(\gamma - \Delta\mu/\mu)^2$, respectively. The new term has a sixfold symmetry like the bunching; the imaginary character indicates that the size of the magnetic moment ordered in the plane is modulated as in Fig. 4(c).

The question arises as to whether the empirical expression (12) is unique in explaining the difference in the reduced intensities of the fifth- and seventh-order satellites, or if phase modulations in the plane of the spiral could yield the same result. Even if Eq. (12) is valid, it simply states that the projection of the magnetic moments in the

plane of the spiral is not equal for all directions. Assuming that all the holmium magnetic moments are equal to their maximum value at low temperature, new modulations of the magnetic structure should appear along the c axis. In Appendix A we discuss the diffraction consequences of the required structural modulations which would give rise to additional satellites of sufficient intensity to be readily observable. Indeed the spiral structure, with its sensitivity to perturbative forces, constitutes a crystallographer's delight.

The outcome of the crystallographic exercise is that no evidence for the missing moments of Eq. (12) is found in the diffraction pattern, and we conclude that the fluctuation $\Delta\mu/\mu$ of the magnetic moments is a real effect. The origin of the moment defect could be attributed to the crystal field. However, the difference in the size of the moments, pointing along the easy and hard axes of the hexagonal plane is a third-order effect in the crystal field. Instead, the observed moment defect can be understood in terms of the zero-point motion. A recent calculation,[11] using approximate values for the exchange and anisotropy constants, yields a moment defect of the same order of magnitude as that observed experimentally. (A tilted spiral structure has been proposed as a stable configuration between the spiral and conical phases of holmium.[12] We examine the neutron-diffraction evidence for such a phase in Appendix B.)

To calculate the magnetic form factor with Eq. (1) numerical values for the $\langle j_{2n}\rangle$ integrals are needed. Three evaluations of $U(r)$ in Eq. (2) are presently available. The first values for the $\langle j_{2n}\rangle$ integrals obtained from Hartree-Fock nonrelativistic wave functions[4] are shown in Fig. 1. The second set of values may be derived self-consistently from the intensities of the structural satellites,[13,14] and uses the same basis functions as used for the Hartree-Fock scheme. The third set is based on relativistic Dirac-Fock wave functions.[15] All three sets of $\langle j_{2n}\rangle$ integrals are very similar, especially for $\sin\theta/\lambda < 0.6$ Å^{-1}, and we have used the Dirac-Fock values. The quantum effect of the zero-point motion, if introduced rigorously, would require the complete reanalysis of the form factor. Even then, an adequate knowledge of the amplitude of vibration of the spin both in, and normal to, the hexagonal plane would be necessary.[11] Stringfellow *et al.*[16] have pointed out that the stability conditions for the spiral-to-cone transition requires K_2, the axial anisotropy, to change sign. At some point, therefore, the value of K_2 must be small and the motion of the spins is presumably mainly out of the basal plane.[17] In our model of the magnetic structure, we have assumed such a motion is responsible for producing the moment defect, although the effect of the zero-point motion on the intensities of the third-order satellites is very small.

TABLE IV. Observed and calculated $|F|^2$ values (in units of 10^{-24} cm^2) for $Ho_{0.9}Sc_{0.1}$ at 5 K. The observed values are averaged over equivalent reflections. [They are corrected for extinction and absorption and normalized to the nuclear reflections by taking $\bar{b} = 0.88 \times 10^{-12}$ cm.] The calculated values are given by assuming $\mu = 9.7\mu_B$, $\mu_F = 1.57\mu_B$, $\gamma = 0.15$, $\Delta\mu/\mu = 0.03$, and the relativistic Dirac-Fock form factor.

Reflection	$\lvert F\rvert^2_{obs}$	$\lvert F\rvert^2_{calc}$
(00.2)	0 ± 0.05	0
(11.0)	0.30 ± 0.02	0.30
$(00.2)^{-1}$	8.26 ± 0.37	8.95
$(00.2)^{+1}$	7.65 ± 0.23	8.04
$(00.4)^{-1}$	4.67 ± 0.22	4.88
$(00.4)^{+1}$	3.83 ± 0.24	4.08
$(00.6)^{-1}$	1.98 ± 0.10	2.07
$(00.6)^{+1}$	1.57 ± 0.08	1.66
$(11.0)^{+1}$	2.90 ± 0.06	2.99
$(11.2)^{-1}$	3.04 ± 0.07	3.12
$(11.2)^{+1}$	3.01 ± 0.07	3.05
$(22.0)^{+1}$	0.72 ± 0.10	0.74
$(00.4)^{-5}$	0.060 ± 0.005	0.057
$(00.2)^{+5}$	0.046 ± 0.005	0.052
$(00.6)^{-5}$	0.029 ± 0.003	0.028
$(00.4)^{+5}$	0.018 ± 0.003	0.025
$(11.2)^{-5}$	0.023 ± 0.002	0.025
$(11.0)^{+5}$	0.026 ± 0.002	0.025
$(22.2)^{-5}$	0.007 ± 0.001	0.007
$(22.0)^{+5}$	0.006 ± 0.001	0.006
$(00.2)^{+7}$	0.019 ± 0.002	0.017
$(00.6)^{-7}$	0.016 ± 0.003	0.012
$(00.4)^{+7}$	0.009 ± 0.002	0.006
$(11.2)^{-7}$	0.010 ± 0.001	0.011
$(11.0)^{+7}$	0.011 ± 0.001	0.011
$(11.4)^{-7}$	0.011 ± 0.001	0.011
$(11.2)^{+7}$	0.007 ± 0.001	0.009

We are now in a position to calculate the magnetic intensities and compare these quantitatively with the experimental results. The effects of bunching and the moment reduction are incorporated by using Eq. (12). In practice it is easier to treat these complications within the framework of a commensurate lattice. Such a procedure is always possible by representing the periodicity of the spiral as the ratio of two integers (5/27 for Ho at low temperature and 3/13 for $Ho_{0.9}Sc_{0.1}$). The calculation then requires that the direction of the first magnetic moment be fixed, thus lifting the degeneracy of the spiral. However, as expected, arbitrary variations of the phase angle do not change the intensities of the diffraction lines. The

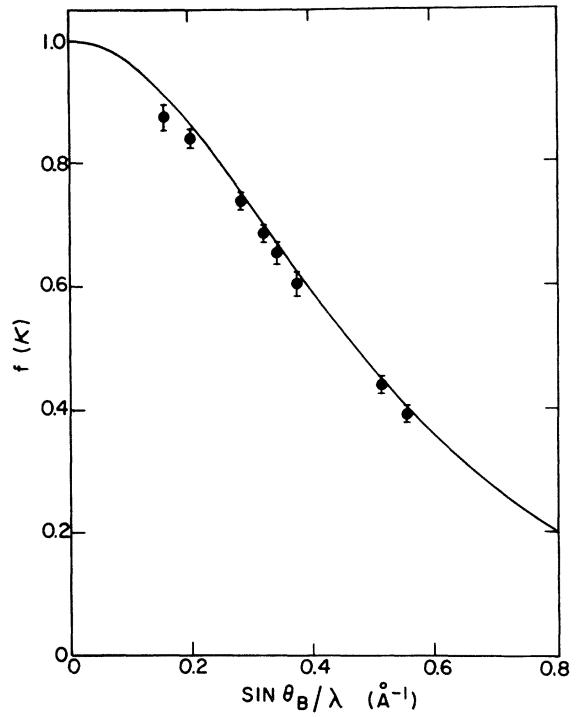

FIG. 6. Experimental form factor, as derived from the intensities of the main satellites at 5 K, and the relativistic Dirac-Fock form factor (Ref. 15) derived for reflections along c^*, i.e., $\beta = \pi/2$.

calculated intensities of the structural satellites from $Ho_{0.9}Sc_{0.1}$ are compared with experiment in Table IV. In Fig. 6 we present an experimental form factor derived from the intensities of the structural satellites, together with the theoretical Dirac-Fock form factor. The over-all agreement is good, except for the first two reflections, which have the largest extinction corrections.

IV. EXPERIMENTAL ASPHERICITY

In Table V we present the experimental values of $|F|^2$ for the third-order satellites, which arise from the aspherical magnetization density, for $Ho_{0.9}Sc_{0.1}$ and Ho. They are compared with values calculated in Sec. II, but with the structural model described in Sec. III. The $\langle j_{2n} \rangle$ functions are those of Freeman and Desclaux,[15] and the angular factors c_i are for the lowest state of holmium, $M = 8{:}^5I_8$. The experimental $|F|^2$ values are approximately 50–100% greater than the calculated.

To display the data visually we reduce the experimental data to an effective $\langle j_{2n} \rangle$ and compare with the theoretical $\langle j_2 \rangle$ function. The structure factor can be written

$$|F|^2_{hhl^{\pm 3}} = \tfrac{1}{4}[(\tfrac{1}{2} - \tfrac{3}{4}\gamma)^2 \sin^2\theta + (\tfrac{1}{2} + \tfrac{3}{4}\gamma)^2] \times [0.54c \cos^2\theta \times 1.749(\langle j_2 \rangle + \cdots)]^2 \times 10^{-24} \text{ cm}, \quad (13)$$

where c is the holmium concentration and θ is the inclination of the scattering vector from the basal plane. In Eq. (13), the small effects of the moment reduction are neglected, although the entries in Table V take this into consideration. Equation (13) contains terms in $\langle j_4 \rangle$ and $\langle j_6 \rangle$, although they do not contribute more than ~5% of the contribution from $\langle j_2 \rangle$. As an *approximation*, therefore, we look on the third-order satellite as arising from the $\langle j_2 \rangle$ function only, and a comparison with the theoretical $\langle j_2 \rangle$ function is presented in Fig. 7. (The entries in Table V do not use this approximation.) The over-all κ dependence of the data is in agreement with theory and is drastically different from that of the structural satellites (see Fig. 6). However, the intensities of the third-order satellites (Table V) of holmium and, even more of $Ho_{0.9}Sc_{0.1}$, are larger than those predicted by the single-ion theory.

The most trivial explanation for the discrepancy is that the third-order satellites arise partially from structural modulations. Summarizing the results of Appendix A, a third-order modulation of the magnetic moments in the hexagonal plane would give rise to $00l^{\pm 3}$ satellites, which are defi-

TABLE V. Observed and calculated $|F|^2$ values of the third (asphericity) satellites at 5 K, expressed in units of 10^{-27} cm^2. Note the change of scale of 10^{-3} compared to Table IV.

Reflection	$\frac{\sin\theta_B}{\lambda}$	$Ho_{0.9}Sc_{0.1}$ $\|F\|^2_{obs}$	$Ho_{0.9}Sc_{0.1}$ $\|F\|^2_{calc}$	Ho $\|F\|^2_{obs}$	Ho $\|F\|^2_{calc}$
$(00.0)^{+3}$	0.062	0 ± 0.05	0	0 ± 0.005	0
$(11.0)^{+3}$	0.289	2.0 ± 0.2	0.82	1.7 ± 0.2	1.01
$(11.2)^{-3}$	0.306	2.1 ± 0.2	0.80	1.4 ± 0.2	0.97
$(11.2)^{+3}$	0.372	1.6 ± 0.2	0.66	1.6 ± 0.2	0.85
$(11.4)^{-3}$	0.409	1.7 ± 0.4	0.59	0.7 ± 0.3	0.72
$(11.4)^{+3}$	0.506	0.6 ± 0.3	0.40		
$(22.0)^{+3}$	0.569	4.8 ± 0.3	3.02	4.4 ± 0.3	3.71
$(22.2)^{-3}$	0.577	4.3 ± 0.3	2.93		

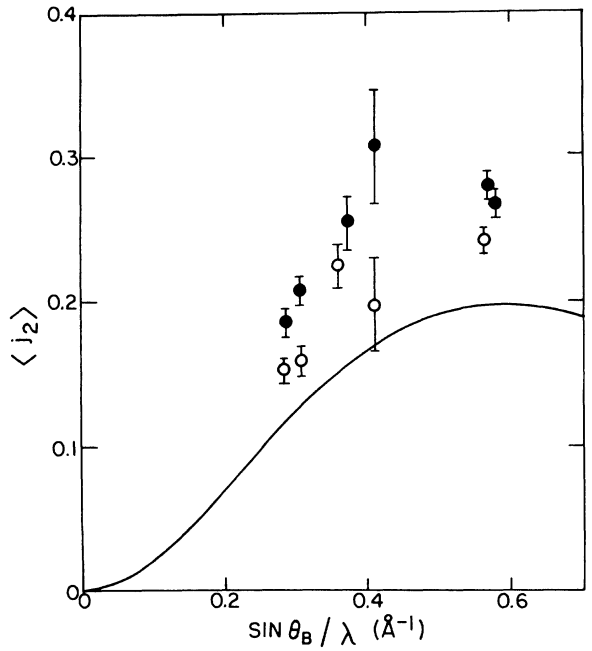

FIG. 7. Relativistic Dirac-Fock $\langle j_2 \rangle$ term compared with the effective $\langle j_2 \rangle$, as given by Eq. (13), derived from the intensities of the third-order satellites. The open points refer to Ho; the closed to $Ho_{0.9}Sc_{0.1}$.

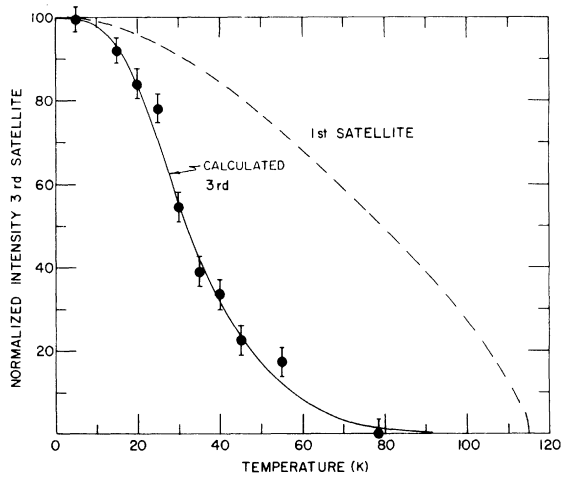

FIG. 8. Temperature dependence of the $(220)^{+3}$ satellite for $Ho_{0.9}Sc_{0.1}$. The curve drawn through the experimental points represents the behavior predicted on the basis of the molecular-field theory, using the intensity of the first satellite to derive the magnetization.

nitely not present. A third-order modulation of the magnetic moments along the c axis is less easy to reject, since the intensities generated would have a dependence on the azimuthal angle θ very similar to that of the satellites arising from the asphericity. However, the form factor of such structural satellites would be similar to that in Fig. 6. As shown in Fig. 7 the discrepancy between theory and experiment is essentially independent of κ and cannot be accounted for by a simple structural modulation.

An alternative explanation of the discrepancy in Fig. 7 is that the incorrect form factor has been used. This, too, is very unlikely. The $\langle j_{2n} \rangle$ integrals are all transforms of the same radial spin density, Eq. (2), and any large change in the $\langle j_2 \rangle$ transform also changes $\langle j_0 \rangle$, etc. Figure 6 shows that the structural satellites agree with the form factor calculated from relativistic Dirac-Fock wave functions, and this agreement implies that the single-electron radial density is in good agreement with theory. Because Fig. 6 basically represents the (large) spherical contribution to the magnetization density, it does not, of course, say very much about the higher-order c_i coefficients, which reflect the (small) aspherical contribution.

A further test of whether the third-order satellites arise entirely from the aspherical magnetization density is to measure their temperature dependence. In Fig. 8 we show the temperature dependence (normalized to the value at 5 K) of the 22.0^{+3} satellite. The intensity of the third-order satellites decreases much more rapidly than the first because the latter varies as $(M/M_0)^2$, whereas the third-order satellite has a temperature dependence approximately represented by $(M/M_0)^8$. The asphericity of the magnetization density is also related to the bulk anisotropy constants, since both are functions of the electronic multipoles of the $4f$ electrons. To calculate the temperature dependence of the third-order satellite we have assumed a free-ion model with a crystal-field interaction which is negligible compared to the exchange interaction. In this simple molecular-field model the magnetic moment stems from the thermal population of the M_J multiplet, which is split into 17 nondegenerate levels by the internal exchange field. The lowest level has $M_J = 8$, giving $\mu = gM_J = 10\mu_B$ per holmium ion, and the next level has $M_J = 7$, etc. The magnetization, or dipole moment, may be derived from the first-order satellite and used to fix the internal exchange field at a given temperature. The resultant asphericity, which is related to higher-order electronic multipoles, is then readily calculated. The temperature dependence is shown in Fig. 8 and is in excellent agreement with experiment. This agreement does not prove necessarily that the c_i coefficients are indeed those of the single-ion theory of holmium (a conclusion which would be in conflict with our findings for the absolute value of the intensities at low temperature); the c_i coef-

ficients simply represent terms in the symmetry of the ion, irrespective of their origin.

V. SUMMARY

In spiral magnetic structures containing aspherical ions, additional satellites, which arise solely from the aspherical contributions to the magnetization density, are found. Such satellites, of which only the third-order are observable, have been measured for Ho and a $Ho_{0.9}Sc_{0.1}$ alloy. The intensities have the correct κ dependence but are stronger than predicted. In investigating this discrepancy, we have made a very careful investigation of the magnetic structures of these materials, leading to some small (but important) modifications of the model proposed by Koehler *et al.*[6] We do not believe the discrepancies in Fig. 7 arise from modulations in the magnetic structure, but are instead a real indication that the magnetization density is *more* aspherical than predicted by the single-ion model. If crystal-field interactions are included, the first-order effect is to reduce the asphericity of the magnetization cloud (because of wave-function admixture) and modify the temperature dependence predicted by the free-ion model. The generally accepted models for the rare-earth metals contain a large exchange term and a relatively weak crystal-field interaction. The agreement in Fig. 8 is consistent with this model.

The discrepancy between the absolute magnitude of the third-order satellite and the theoretical predictions is not surprising in view of our use of such a simple single-ion model. Certainly a more sophisticated approach is needed. For example, in a recent calculation[18] of the spin-density distribution in gadolinium, which is usually considered a spherically symmetric ion, small aspherical terms are predicted. The role of conduction electrons[14] has also been completely neglected in our calculations. We may speculate, for example, that the interaction between the conduction electrons and the localized $4f$ moments might lead to an increase in the asphericity. Quite apart from the conduction-electron effects we must also consider multipole interactions between the $4f$ electrons.[19] Such interactions may change the magnetization density, although a quantitative calculation of such effects represents a formidable task.

ACKNOWLEDGMENTS

We would like to thank T. O. Brun for participating in the early discussions that led to the experiment, and for collecting some of the data on holmium. We are indebted to J. Robinson for his advice on the form-factor analysis and to A. J. Freeman for the relativistic integrals.

APPENDIX A: A CRYSTALLOGRAPHER'S DELIGHT

Modulations in the plane of the spiral. The magnetic spiral structure has a period $\vec{\tau}$. In general, we may consider any type of modulation with period $\vec{\tau}$ as commensurate with the lattice, in the sense that it is experimentally impossible to distinguish a truly incommensurate magnetic structure from one for which n_0 magnetic periods are exactly contained in n_0 crystal cells. (In the case of the hcp crystals and structures we are considering here, with $\vec{\tau} \| \vec{c}$, n_0 crystal cells imply $2n_0$ layers.) For example, at low temperature, for Ho (annealed) $n_0 = 27, m_0 = 5$, and for $Ho_{0.9}Sc_{0.1}$, $n_0 = 13, m_0 = 3$, within our resolution. Let us now consider reflections only along the c^* axis, and index them as $00l$ relative to the large unit cell of $2n_0$ layers. Let us consider the origin of the cell to lie at $(0, 0, -c/4)$. Then the structure factor for the magnetic $00l$ reflection is

$$\vec{F} \propto f \sum_{n=0}^{2n_0-1} \vec{\mu}_n \exp 2\pi i \left((n+\tfrac{1}{2}) \frac{l}{2n_0} \right), \tag{A1}$$

where f is the form factor, and $\vec{\mu}_n$ is the moment in the nth layer, given by

$$\vec{\mu}_n = \frac{\vec{\mu}_x - i\vec{\mu}_y}{2} \exp 2\pi i \left((n+\tfrac{1}{2}) \frac{m_0}{2n_0} + \delta_n \right) + \text{c.c.} \tag{A2}$$

$\vec{\mu}_x$, $\vec{\mu}_y$ are unit vectors along the x and y axes, respectively, and $2\pi\delta_n$ represents the deviation (in the plane of the spiral) from the pure spiral arrangement. Taking into account the symmetry property, $\delta_n = \delta_{2n_0-1-n}$, Eqs. (A1) and (A2) can be combined to give

$$\vec{F} \propto f \Bigg[(\vec{\mu}_x - i\vec{\mu}_y) \sum_{n=0}^{n_0-1} \cos 2\pi \left((n+\tfrac{1}{2}) \frac{m_0 + l}{2n_0} + \delta_n \right) + (\vec{\mu}_x + i\vec{\mu}_y) \sum_{n=0}^{n_0-1} \cos 2\pi \left((n+\tfrac{1}{2}) \frac{m_0 - l}{2n_0} + \delta_n \right) \Bigg]. \tag{A3}$$

It is now possible to determine the relations between the squares of the structure factors for peaks with different l. Writing $I = (\vec{F} \cdot \vec{F}^*)/f^2$, we obtain

$$I_l = P(m_0 + l) + P(m_0 - l), \tag{A4}$$

where

$$P(m_0 + l) = \left[\sum_{n=0}^{n_0-1} \cos 2\pi \left((n+\tfrac{1}{2}) \frac{m_0 + l}{2n_0} + \delta_n \right) \right]^2$$

and

$$P(m_0 - l) = \left[\sum_{n=0}^{n_0-1} \cos 2\pi \left((n+\tfrac{1}{2}) \frac{m_0 - l}{2n_0} + \delta_n \right) \right]^2.$$

We also have

$$P(m_0 + l) = P(m_0 + l + 2n_0)$$

and

$$P(m_0 + l) = P(-m_0 - l).$$

Now, a satellite of order r in the conventional notation may be related to its index l with respect to our large unit cell, by

$$l = rm_0 + 2sn_0 \quad (r, s \text{ both integers}).$$

Using this and the above relations, it may be shown that

$$I_{5\text{th}} = P(6m_0) + P(4m_0)$$

and

$$I_{7\text{th}} = P(8m_0) + P(6m_0). \tag{A5}$$

All the terms in Eq. (A5) are positive. Hence $I_{5\text{th}} \simeq 2I_{7\text{th}}$ only if $P(4m_0)$ is greater than both $P(6m_0)$ and $P(8m_0)$. But the term $P(4m_0)$ appears in the expression for the *third*-order satellites along $00l$, and such satellites were absent for both $Ho_{0.9}Sc_{0.1}$ and Ho.

Modulations normal to the plane of the spiral. The conservation of the magnetic moment requires that

$$\mu_z^2 = \mu^2 - \mu_\perp^2, \tag{A6}$$

where μ_z and $\mu_\perp$ are moments parallel and perpendicular to the c axis, respectively. From Eq. (12)

$$\mu_\perp = \mu[1 - (\Delta\mu/\mu)(1 + \cos 6\phi_2^0)]. \tag{A7}$$

Equation (A6) has two solutions approximately given by

$$\mu_z = 2(\mu\Delta\mu)^{1/2}\cos 3\phi_L^0, \tag{A8}$$

$$\mu_z = 2(\mu\Delta\mu)^{1/2}\left|\cos 3\phi_L^0\right| = \frac{4(\mu\Delta\mu)^{1/2}}{\pi}(1 + \tfrac{1}{3}\cos 6\phi_0 + \cdots). \tag{A9}$$

The magnetic structures corresponding to the two models have the shape of corrugated roofs; in the model given by Eq. (A8) the concavities are alternatively up and down, and the solution is antiferromagnetic. The oscillation of the moments along the z axis has a period 3τ, and the maxima of the oscillations occurs for the moments along the hard directions in the hexagonal plane. The second solution, Eq. (A9) corresponds to a corrugated roof with the concavities in one direction only and gives a ferromagnetic component, with $6n$th-order satellites.

To conserve the magnetic moment of $\sim 10\mu_B$ with the moment defect observed in the plane [$(0.2-0.3)\ \mu_B$], we should observe satellites with amplitudes proportional to $\sim 2\mu_B$ [see Eq. (A6)]. These satellites should be at least as large as the fifth satellites. However, no additional satellites were observed by us or by Koehler *et al.*[6]

One of the modulations proposed, Eq. (A8), has the same periodicity (3τ) as the main asphericity satellites. If even a small modulation of such character were present, the intensities of the asphericity satellites would be greatly perturbed. The angular dependence of the intensity of the sinusoidal modulation along the c axis is $\cos^2\theta$, whereas the angular dependence of the intensity of the third-order satellite, due to the asphericity of the magnetization density, is approximately $\cos^4\theta$, and thus the two types of satellites are not readily distinguishable by their dependence on the azimuthal angle θ. However, the form factor for the two types of effects are completely different so that to distinguish between them one must collect data over a range of κ values.

APPENDIX B: IS THE HOLMIUM SPIRAL TILTED?

The model presented in this paper, that the magnetic structure at 4.2 K of holmium and $Ho_{0.9}Sc_{0.1}$ is a cone, with its axis parallel to the c axis, is commonly accepted in the literature. However, a simple conical structure cannot pass continuously to a spiral structure.[20] Sherrington[12] has shown that if the single-ion anisotropy parameter K_2 varies smoothly with the temperature, the transition between the cone and spiral structure occurs via an intermediate phase, in which the direction of propagation of the spiral remains parallel to the c axis, but the plane containing the magnetic moments is no longer perpendicular to the c axis. Sherrington[12] discussed several modulations of such a tilted spiral structure, one of which gives rise to third-order satellites along the c axis. Support for such a model has been inferred from the results of recent ultrasonic experiments on holmium.[21] At 24 K a peak in the absorption was found that was well separated from the peak at 20 K associated with the ferromagnetic transition. The absorption peak at 24 K was interpreted as due to the softening of a magnon that occurs when $K_2 = 0$, the extreme for the region of the spiral structure. Hence Tachiki *et al.*[21] concluded that holmium exhibits a tilted magnetic spiral structure between 20 and 24 K.

Neutron-diffraction experiments are capable of determining the tilt of the spiral directly. Since the neutron detects only the component of the magnetic moment normal to the scattering vector, a tilt of the spiral would decrease the intensity of, say, the $(002)^{+1}$ satellites, and would increase the intensity of the $(110)^{+1}$ satellites. The ratio between the intensities of these two satellites is thus sensitive to the tilt of the spiral. For both

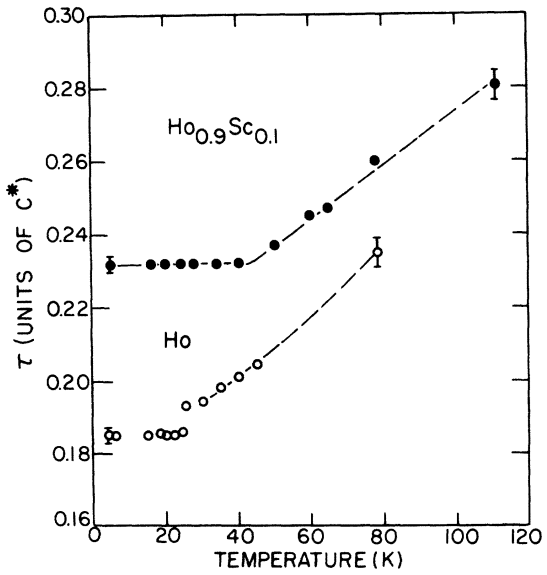

FIG. 9. Variation of the period of the spiral of Ho and $Ho_{0.9}Sc_{0.1}$ with the temperature.

$Ho_{0.9}Sc_{0.1}$ and Ho we did not observe any variation of the ratio I_{002^+}/I_{110^+}. However, this ratio varies quadratically with the tilt angle, with a variation of ~3% for a tilt angle of 10°. This is approximately the precision of our measurements. For pure holmium, we have a single experimental measurement (at 22 K) in the temperature region of interest. Hence we conclude that any tilt of the spiral is less than 10°.

Also of interest is the variation of the spiral periodicity with temperature, as shown in Fig. 9. The temperature dependence for Ho is similar to that given by Koehler *et al.*,[6] except that a low temperature our sample does not become commensurate. A small discontinuity occurs in the periodicity around 25 K, approximately at the same temperature at which the absorption of an ultrasonic shear wave exhibited a maximum.[21] Are the two phenomena connected? Is a spiral—with its infinite phase degeneracy, and a no-gap magnon spectrum[22]—really the magnetic structure that is stable at low temperature?

---

*Based on work performed under the auspices of the U.S. Energy Research and Development Administration.

†Present address: Istituto di Fisica, Università di Genova, Genova, Italy.

‡Present address: Argonne National Laboratory, Argonne, Ill. 60439.

[1]M. Blume, oral presentation at the Sagamore Conference II on Charge and Spin Density, Sagamore, N. Y., 1967 (unpublished).

[2]D. T. Keating, Phys. Rev. 178, 732 (1969).

[3]S. W. Lovesey and D. E. Rimmer, Rep. Prog. Phys. 32, 333 (1969).

[4]M. Blume, A. J. Freeman, and R. E. Watson, J. Chem. Phys. 37, 1245 (1962).

[5]G. H. Lander and T. O. Brun, J. Chem. Phys. 53, 1387 (1970).

[6]W. C. Koehler, J. W. Cable, M. K. Wilkinson, and E. O. Wollan, Phys. Rev. 151, 414 (1966).

[7]H. R. Child and W. C. Koehler, J. Appl. Phys. 37, 1353 (1966); Phys. Rev. 174, 526 (1968).

[8]W. R. Busing and H. Levy, Acta Crystallogr. 10, 180 (1957).

[9]W. H. Zachariasen, Acta Crystallogr. 23, 558 (1967).

[10]G. P. Felcher, Solid State Commun. 12, 1167 (1973).

[11]T. Arai and G. P. Felcher, J. Phys. C 8, 2095 (1975).

[12]D. Sherrington, Phys. Rev. Lett. 28, 364 (1972); J. Phys. C 6, 1037 (1973).

[13]T. O. Brun, G. H. Lander, and G. P. Felcher, Bull. Am. Phys. Soc. 16, 379 (1971).

[14]R. M. Moon, W. C. Koehler, J. W. Cable, and H. R. Child, Phys. Rev. B 5, 997 (1972).

[15]A. J. Freeman and J. P. Desclaux (private communication); see A. J. Freeman and J. P. Desclaux, Int. J. Magn. 3, 311 (1972), for a similar calculation for gadolinium.

[16]A. D. B. Woods, T. M. Holden, B. M. Powell, and M. W. Stringfellow, Phys. Rev. Lett. 23, 81 (1970); M. W. Stringfellow, T. M. Holden, B. M. Powell, and A. D. B. Woods, J. Phys. C 2, S189 (1970).

[17]T. Egami, J. Phys. C 5, L85 (1972).

[18]B. N. Harmon and A. J. Freeman, Phys. Rev. B 10, 1979 (1974).

[19]R. J. Birgeneau, M. T. Hutchings, J. M. Baker, and J. D. Riley, J. Appl. Phys. 40, 1070 (1969).

[20]B. R. Cooper, R. J. Elliott, S. J. Nettle, and H. Suhl, Phys. Rev. 127, 57 (1962).

[21]M. Tachiki, M. C. Lee, R. A. Treder, and M. Levy, Solid State Commun. 15, 1071 (1974).

[22]R. J. Elliott and R. U. Lange, Phys. Rev. 152, 235 (1966).